ELSEVIER

Journal of Hydrology 260 (2002) 216–230

Journal of Hydrology

www.elsevier.com/locate/jhydrol

Influence of rainfall spatial variability on flood prediction

Patrick Arnaud[a,*], Christophe Bouvier[b], Leonardo Cisneros[c], Ramon Dominguez[c]

[a]*ENGEES, 1 Quai Koch, BP 1039F, 67070 Strasbourg, France*
[b]*IRD, BP 5045, 34032 Montpellier Cedex, France*
[c]*UNAM, Instituto de Ingenieria, CD. Universitaria, Apdo. Postal 70-472, 04510 Mexico D.F., Mexico*

Received 31 October 2000; revised 14 September 2001; accepted 18 December 2001

Abstract

This paper deals with the sensitivity of distributed hydrological models to different patterns that account for the spatial distribution of rainfall: spatially averaged rainfall or rainfall field. The rainfall data come from a dense network of recording rain gauges that cover approximately 2000 km^2 around Mexico City. The reference rain sample accounts for the 50 most significant events, whose mean duration is about 10 h and maximal point depth 170 mm. Three models were tested using different runoff production models: storm-runoff coefficient, complete or partial interception. These models were then applied to four fictitious homogeneous basins, whose sizes range from 20 to 1500 km^2. For each test, the sensitivity of the model is expressed as the relative differences between the empirical distribution of the peak flows (and runoff volumes), calculated according to the two patterns of rainfall input: uniform or non-uniform. Differences in flows range from 10 to 80%, depending on the type of runoff production model used, the size of the basin and the return period of the event. The differences are generally moderate for extreme events. In the local context, this means that uniform design rainfall combining point rainfall distribution and the probabilistic concept of the areal reduction factor could be sufficient to estimate major flood probability. Differences are more significant for more frequent events. This can generate problems in calibrating the hydrological model when spatial rainfall localization is not taken into account: a bias in the estimation of parameters makes their physical interpretation difficult and leads to overestimation of extreme flows.

Keywords: Rainfall variability; Distributed hydrological model; Rainfall fields; Sensitivity; Flood estimation; Mexico

1. Introduction

The objective of this work was to study the sensitivity of distributed hydrological models to the spatial distribution of rainfall, and its influence on the estimation of flood probability. We compare both runoff volumes and peak flows, calculated using either rainfall fields (i.e. hyetographs associated with different spatial observations) or spatially averaged rainfalls (i.e. a synthetic hyetograph obtained by weighted average of the different observations).

Many studies have dealt with the sensitivity of hydrological models together with other uncertainties related to spatial rainfall variability, i.e. with the spatial density of the rain gauge network and with the interpolation methods (Creutin et al., 1980; Kuczera and Williams, 1992; Faurès et al., 1995; Goovaerts, 2000; Wotling et al., 2000); with rainstorm displacement (Surkan, 1974; Gupta and Waymire, 1979; Marshall, 1980; Niemczynowicz, 1987, 1991). These studies show that the spatial distribution of rainfall should be taken into account in any catchment area. It influences not only runoff volumes and peak flows, but also the time shift of hydrographs (Dawdy and Bergman, 1969; Wilson et al., 1979; Troutman,

* Corresponding author. Fax: +33-3-88-24-82-84.
E-mail address: parnaud@engees.u-strasbg.fr (P. Arnaud).

0022-1694/02/$ - see front matter
PII: S0022-1694(01)00611-4

1983; Krajewski et al., 1991). Moreover, it significantly increases uncertainty about the estimation of hydrological model parameters, and consequently estimation of the extreme quantiles (Kuczera and Williams, 1992; Obled et al., 1994).

Studies on the advantages of using rainfall fields as opposed to spatially averaged rainfall are relatively rare. If the sensitivity of the hydrological model to these two patterns of rainfall representation is low, the use of uniform areal rainfall derived from point rainfall distribution combined with the probabilistic areal reduction concept (Brunet-Moret and Roche, 1966; Rodriguez-Iturbe and Mejia, 1974; Lebel and Laborde 1988; Sivapalan and Blöschl, 1998) is justifiable in order to generate design rainfall events. Conversely, it is necessary to generate rainfall fields (Waymire et al., 1984; Smith and Karr, 1985; Bell, 1987; Rodriguez-Iturbe and Eagleson, 1987; Sivapalan and Wood, 1987; Yoo et al., 1996), which are used as probabilized inputs in a distributed hydrological model.

Morin et al. (1995) showed on small Israeli basins how spatial variability of rainfall, obtained by radar, can generate significant variations in flow modeling. Obled et al. (1994), using TOPMODEL for the Real Collobrier 71 km^2 experimental catchment located in southeast France, showed that flows computed using spatially averaged rainfall or rainfall field are not very different. However, as it is generally the case in this type of study, conclusions may be very specific, depending on the scale of the basin, rainfall variability in the area, and the mechanisms involved in the generation of flows.

In this study, rainfall data are from a dense rainfall network located in the Mexico City region. The sensitivity of the distributed model to the rainfall input (spatially averaged or rain field) was studied by comparing the statistics for both peak flows and volumes. To ensure wider application of the conclusions of this study, these comparisons were performed for:

different types of rainfall-runoff conversion models
different sizes of basin
different return periods

The discussion focuses on the suitability to use spatially averaged rainfall combined with areal reduction factor for design rainfall, and on problems that may occur in calibrating the rainfall-runoff models if the spatial organization of rainfall is not taken into account.

2. Methodology

2.1. The study area and the data

The study was carried out in the region around Mexico City, which is characterized by a vast, originally endoreic basin surrounded by several mountain chains. The mean altitude of the basin is 2240 m, but the surrounding mountains often exceed 3000 m and the highest volcanoes reach more than 5000 m (Popocatpetl and Ixatccihuatl, in the southeast). Both the relief and human activities have induced high variability in soils and in land use. On the slopes, vegetation is abundant (pine or eucalyptus woods, extensive pastures or agricultural areas) and andosoils are predominant, while the flat central part of the catchment is characterized by extensive urban areas and plastic clays.

The climate is of the tropical altitude type, characterized by one short rainy season (here from June to September). The mean annual rainfall is approximately 600 mm at an altitude of 2240 m, and up to 1000 mm in the mountains. In spite of the tropical context, the rainfall intensity for short time steps is rather low: for a 10-year return period, rainfall intensity for steps of 5, 60 min and 24 h are, respectively, 164, 46, 2.5 mm/h, with corresponding amounts of 6.8, 46, 60 mm. This is typical of the tropical or equatorial altitude climates in South America, and is comparable to other sites like Quito (Ecuador), La Paz (Bolivia) (Bouvier et al., 1999).

Rainfall records came from a rain gauge network covering an area of nearly 2500 km^2, and during the period 1988–1998, included 49 tipping bucket rain gauges. Five recording rain gauges were judged to be substandard and were discarded from this study.

Rain events were delimited in time by the absence of rainfall for a period of at least 1 h at all the stations. The duration of the events range between 9 and 126 h (median 40 h), while maximal rainfall depths vary up to 172 mm. The spatial correlations between point cumulative rainfalls can be expressed through the climatologic variogram, which can be fitted to a spherical model (no nugget effect, sill = 1.25,

Table 1
Characteristics of the sample of 50 rain events

	Median	Minimum	Maximum
Duration (h)	40	9	126
Local maximum cumulative rainfall (mm): PMAX	85.8	70.1	172.2
Cumulative basin rainfall (mm): PBAS	21.9	2.0	80.7
R = PMAX/PBAS	3.4	1.54	20
CV_S median	0.73	0.27	3.03
Rainfall gauges number where $P >$ PMAX/2	4	1	33

range = 30 km). To give some idea of the spatial extent of the rain fields, the mean area of the 10 mm isohyet is about 500 km^2 (Cisneros et al., 1998).

We finally retained the 50 most significant events to form our reference sample, which will be used as input data for the distributed hydrological model. These events are those with a rainfall depth of at least 70 mm at one of the stations. Some characteristics of the sample are given in Table 1.

The cumulative basin precipitation (PBAS) was calculated by using the Thiessen polygon method:

$$\mathrm{PBAS} = \sum_{i=1}^{N} \alpha_i P_i$$

where α_i is the Thiessen coefficient associated to i station, P_i the cumulative rainfall at the i station, and N the number of recording stations.

The spatial coefficient of variation (CV_S) was defined by:

$$\mathrm{CV_S} = \frac{\sqrt{\sum_{i=1}^{N} \alpha_i (P_i - \mathrm{PBAS})^2}}{\mathrm{PBAS}} \quad (1)$$

The spatial extent of rainfall may differ considerably from one event to another: some are very localized and others cover the whole catchment area, as shown in Fig. 1. The first event is a local rain event, which mainly affects only one station and which represents the highest maximum local cumulative rainfall (PMAX = 172.2 mm; PBAS = 27.5 mm) observed. The second event is a widespread rain event, which affects the whole of the study area and represents the highest cumulative basin rainfall (PMAX = 140.2 mm; PBAS = 80.7 mm) observed.

2.2. The hydrological models

MERCEDES (Bouvier et al., 1994; Bouvier and Delclaux, 1996), is a modeling toolkit, that contains a wide variety of conceptual or physically based

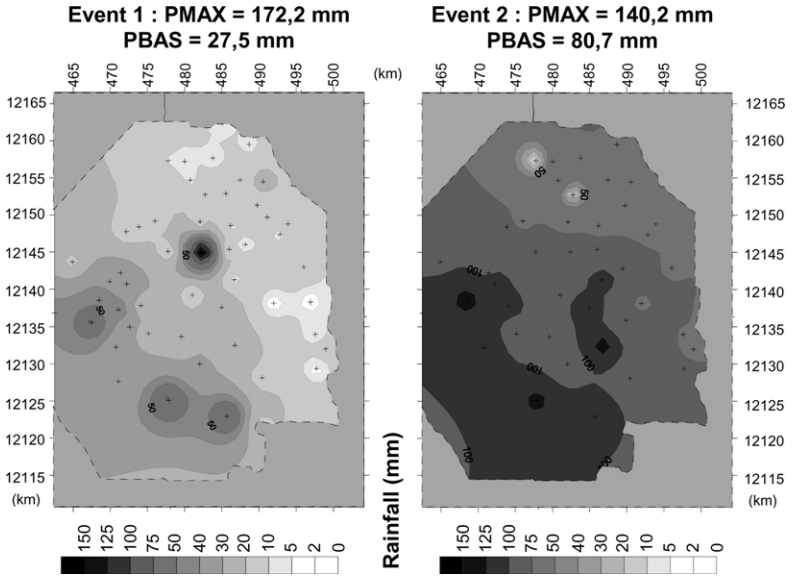

Fig. 1. Maps of the isohyets of two extreme events.

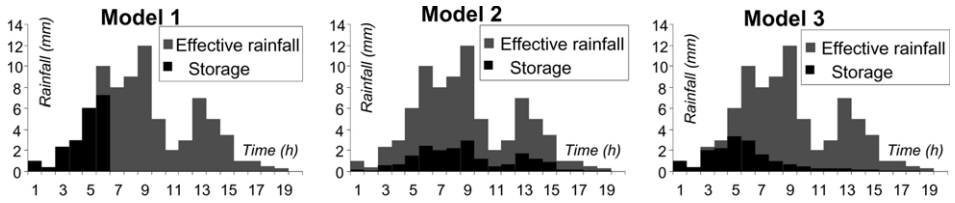

Fig. 2. Influence of the runoff production model on runoff.

rainfall-runoff models. All of them operate with a discretization of the catchment into regular grid squares whose size is defined by the user (in our case, grid mesh length varied from 30 to 250 m, see Section 2.3). The precipitation $P_{m,t}$ received by each grid mesh (m) at time step (t) is interpolated in space from the observed hyetographs (see Section 2.4). For each grid mesh (m) and each time step (t), the effective precipitation $\mathrm{Pe}_{m,t}$ that contributes to runoff is calculated using different runoff production models. In this study, we tested successively three runoff production models coupled with the same routing model. To render further analysis more readable, each of the production models accounts only for one parameter, but their different features may describe a rather broad range of hydrological behaviors.

Model 1 (complete interception): runoff begins after the cumulative rainfall exceeds a threshold value STO (in mm). Afterwards, the whole excess cumulative rainfall is converted into runoff. This model enables runoff due to soil saturation in water.

$$\mathrm{Pe}_{m,t} = 0 \qquad \text{if } \sum_{j=0,t} P_{m,j} < \mathrm{STO}_m$$

$$\mathrm{Pe}_{m,t} = P_{m,t} \qquad \text{when } \sum_{j=0,t} P_{m,j} > \mathrm{STO}_m$$

Model 2 (constant storm-runoff coefficient): effective precipitation is directly proportional to precipitation intensity. W_m (proportionality factor) can be interpreted as a constant storm-runoff coefficient over time. It can be considered for example as the imperviousness coefficient of an urban catchment.

$$\mathrm{Pe}_{m,t} = W_m P_{m,t}$$

Model 3 (partial interception): this is an intermediate case between models 1 and 2. Rainfall first fills a reservoir with a storage capacity STO (in mm), as in Model 1, but this reservoir has a continuous discharge that produces additional runoff. Discharge is a function of both the level of the reservoir at the beginning of the time interval and the intercepted rainfall. It can be considered as a variable storm-runoff coefficient whose value increases with the reservoir level, and varies from 0 to 100%:

$$\mathrm{Pe}_{m,t} = P_{m,t}\frac{\lfloor 2\mathrm{stoc}_{m,t} + P_{m,t}\rfloor}{2\mathrm{STO}_m}$$

$$\text{if } P_{m,t} \le \mathrm{STO}_m - \mathrm{stoc}_{m,t}$$

$$\mathrm{Pe}_{m,t} = (P_{m,t} - (\mathrm{STO} - \mathrm{stoc}_{m,t})) + (\mathrm{STO} - \mathrm{stoc}_{t,m}) \times \frac{\lfloor 2\mathrm{stoc}_{m,t} + (\mathrm{STO} - \mathrm{stoc}_{t,m})\rfloor}{2\mathrm{STO}_m}$$

$$\text{if } P_{m,t} > \mathrm{STO}_m - \mathrm{stoc}_{m,t}$$

where $\mathrm{stoc}_{m,t}$ being the filling level of the reservoir at time step t. This level was fixed arbitrarily at zero at the beginning of the rain event.

This model enables some decreasing infiltration, which can be compared to the transitory phase of a Hortonian process. In this case, the final infiltration tends towards zero. It must also be noted that the soil reservoir level cannot decrease during a given event, which means that neither percolation into the deep aquifer nor evapotranspiration are taken into account at the event scale (this concerns both the models 3 and 1). This would have been of course possible, but to ensure the clarity of the analysis, we preferred the models we use to be as simple as possible. The influence of this simplified assumption is further discussed in Section 4.

The graphs in Fig. 2 show the responses of the three runoff production models subjected to a total rainfall of 80 mm and parameterized in order to generate an effective rainfall close to 60 mm. The corresponding

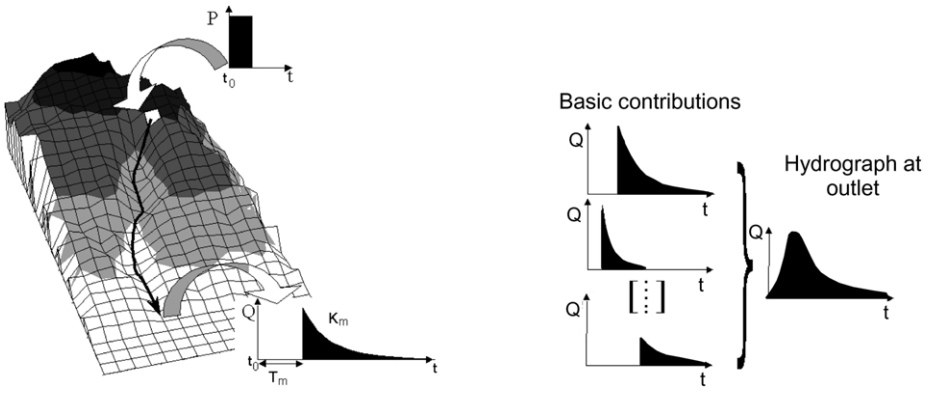

Fig. 3. Routing model.

parameters are STO = 20 mm for Model 1, $W = 0.75$ for Model 2 and STO = 30 mm for Model 3.

For a given grid mesh at a given time, each elementary runoff contribution is then routed to the outlet, using a lag and route model. The model needs two estimates (Fig. 3):

travel time T_m from the grid mesh to the outlet, which is expressed by $T_m = \sum_{i=1,k} L_i/V0_i$, where k is the number of grid mesh traveled between the grid mesh (m) and the outlet, L_i and $V0_i$ are the length and the flow celerity associated with each grid mesh (i).

storage capacity K_m during the travel time, which has units in time and corresponds to the parameter of a linear storage model (Chocat, 1997, p. 867; Maidment, 1993, pp. 26–29). It is assumed that K_m may be related to the travel time T_m by a linear function $K_m = K0_m T_m$, where $K0_m$ is a non-dimensional characteristic of the grid mesh (m).

So the routing model is fully determined by the V0 and K0 values of each grid mesh. At the outlet, the elementary hydrograph due to an effective rainfall $Pe_{m,t}$ of a mesh (m) over time $[t_0; t_{0+\Delta t}]$, is expressed by:

$$Q(t) = 0 \qquad \text{if } t < t_0 + T_m$$

$$Q(t) = Pe_{m,t}/K_m \, e^{-(t_0+T_m-t)/K_m} \qquad \text{if } t > t_0 + T_m$$

The complete hydrograph results from the addition of the elementary hydrographs provided by each grid mesh at each time step. It must be noted that the V0 celerity does not change with time, therefore the travel time to the outlet is invariant for a given mesh. This implies the same linearity properties as those of the unit hydrograph, of which our routing model can be considered as a distributed form.

2.3. Reference basins

Four fictitious basins of different surface areas were defined. In order to mainly study the influence of spatial rainfall information, several simplified assumptions were made.

First, we chose to conserve the same morphology for all four basins. This was performed by applying various reduction ratios to the grid mesh area: 1/1 for the largest basin, then roughly 1/2, 1/4 and 1/8. The number of grid squares remains the same for all four basins (176×232), but their size varies from 250 to 125, 65 and 30 m basins 1–4, respectively, and their surface area is thus, respectively, 1531, 383, 103 and 22 km^2. Next, these basins were located in the study zone in such a way as to include both the highest number of recording rain gauges and the strongest rainfalls (Fig. 4), in order to grab the highest possible spatial variability of the most significant rainfalls. Although very artificial, this method allowed to minimize the sample effects due to irregular network density or localized extreme events.

Second, the basins are considered to be spatially homogeneous, i.e. both the runoff production conditions (parameters STO or W) and the routing conditions (parameters V0 and K0) are constants on all grid meshes. The initial humidity conditions are also

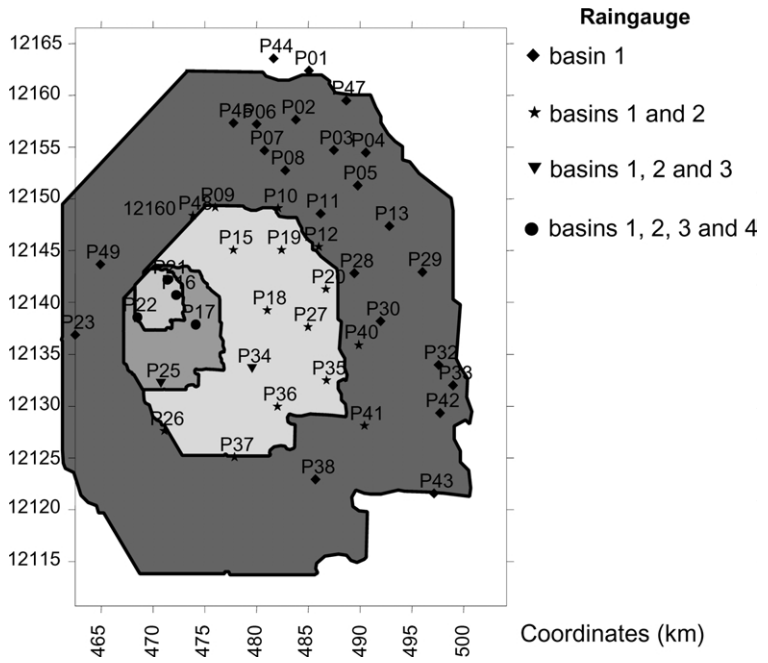

Fig. 4. Location of recording rain gauges and basin limits.

considered to be spatially homogeneous. Events are assumed to be independent, and initial humidity conditions here correspond to dry conditions.

2.4. Tests

The different tests consisted in comparing the flows calculated according to the two patterns of rainfall input used by the distributed hydrological model: uniform basin rainfall (UR: 'uniform rainfall') and rainfall field (NUR: 'non-uniform rainfall'). The first, UR, is represented by a synthetic hyetograph obtained by the weighted average of different hyetographs observed in space. This synthetic hyetograph is calculated for each time step using the Thiessen coefficients, and each mesh of the basin receives the same quantity of rainfall. The second, NUR, is represented by the different hyetographs observed in space; the rainfall received by each mesh is that of the nearest station (hypothesis of Thiessen polygon method). Other methods were tested for the construction of uniform rainfall (centered hyetograph method shifted in time in order to have the maximum intensities coincide), as well as other modes of spatial interpolation (weighted inverse distance, spline function, kriging). However, these methods did not significantly modify the conclusions of the study; this can be explained by a sufficient network density (Cisneros et al., 2000). Thus the simplest method, mentioned earlier, was adopted.

Tests were carried out for different models, different basin sizes, different time steps, and different parameter values. In each case, the tests consisted of comparing the empirical distribution of runoff volumes and peak flows, calculated for the 50 rain events as a function of either uniform or non-uniform patterns of the rainfall variability. The empirical cumulative frequencies were calculated by Hazen formula: $F(X_i) = (i - 0.5)/n = \text{Probability}(X \leq X_i)$, where i indicates the rank of the observation x_i ranked in ascending order, and n the total number of observations ($n = 50$).

The comparison of the empirical distributions was then expressed using the relative errors between the quantiles of the same rank, calculated in the following way:

$$E_i(\%) = \frac{X_{\mathrm{UR}_i} - X_{\mathrm{NUR}_i}}{X_{\mathrm{NUR}_i}} \times 100 \qquad (2)$$

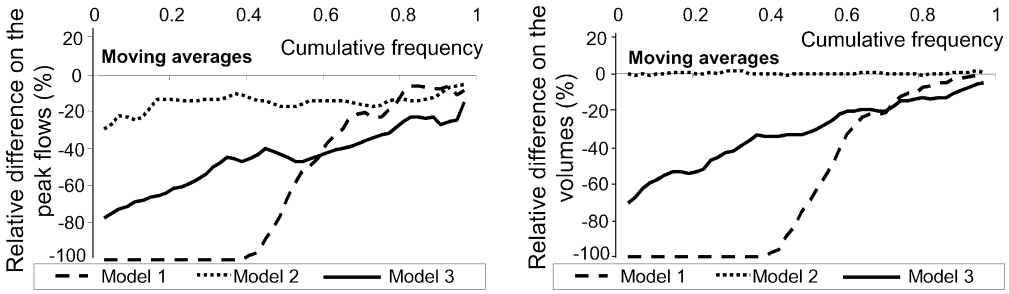

Fig. 5. Relative errors on the quantiles of peak flows and runoff volumes calculated from a UR and a NUR: influence of the runoff production model.

where X_{UR} and X_{NUR} are the values of the quantiles resulting from the distribution of the peak flows (or runoff volumes) calculated from the UR and from the NUR, respectively.

3. Results

3.1. Influence of model type

In this part, the models were applied to the largest basin ($S = 1531$ km^2). Calculations were carried out at an hourly time step.

3.1.1. Influence of the runoff production model

The runoff production parameter was fixed at STO = 20 mm for Model 1, $W = 0.75$ for Model 2 and STO = 30 mm for Model 3 (see example in Section 2.2, Fig. 2). These values guarantee the same mean rainfall-runoff coefficient for the 50 studied events. The routing parameters were fixed at V0 = 1 m/s and K0 = 0.7 for each grid mesh. These values are considered to be suitable in the studied area (Bouvier et al., 1994).

For each of the three runoff production models, coupled with the same routing model, the empirical frequency distributions of the peak flows and the runoff volumes were calculated from the sample of 50 rain events. The relative errors (E_i) defined in Eq. (2) were calculated for the different models of runoff production. They were drawn against the corresponding cumulative frequency $(i - 0.5)/50$ (Fig. 5). To facilitate the interpretation of results, we have smoothed the curves by a moving average calculated on three values (Fig. 5).

Modeling based on runoff production by a constant runoff coefficient (Model 2), is not very sensitive to the spatial distribution of rainfall. Errors in runoff volumes are very small, and may even be zero for most of the cumulative frequencies. This can be explained, in this particular case, by the linearity of the transformation of precipitation into effective rainfall. Thus, the overestimation of peak flows obtained with NUR is only due to the effect of the position of storm cells on the effective rainfall routing. This effect generates errors ranging from −20 to −10% on peak flow quantiles resulting from the two patterns of rainfall representation.

In contrast, runoff production by surpassing of a threshold on cumulative rainfall (Model 1), may strongly underestimate peak flows and runoff volumes calculated using a uniform rainfall. The errors are maximum (−100%) for 21 events, for which the flows calculated with UR are zero. For these events, smoothing due to the spatial average rainfall is significant, and the cumulative uniform rainfall does not exceed the imposed threshold (here, 20 mm), whereas this threshold may be exceeded locally in several places. Such events are generally not very widespread events. For more significant flows, the spatial average rainfall exceeds the imposed threshold and the rainfall excess fully participates in the runoff. Furthermore, when rainfall considerably exceeds the imposed threshold, Model 2 acts like Model 1, with a runoff coefficient close to 100%, and that is the reason why we find similar errors of around −10% in both models. Finally, results obtained with Model 2 are quite different, but it is worth noting that in the case of an extreme event, the differences resulting from using UR and NUR are not very great.

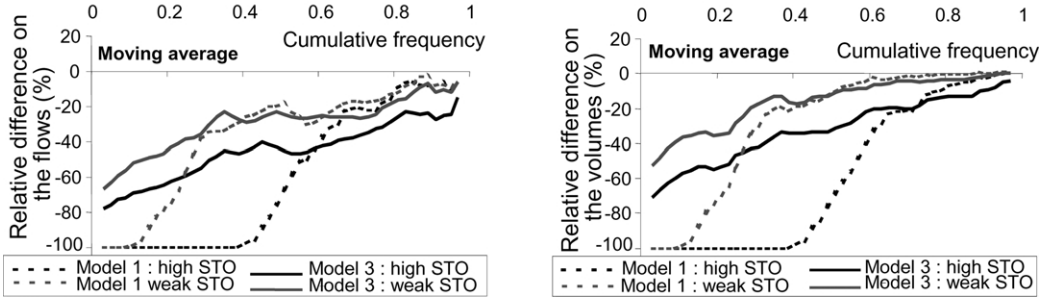

Fig. 6. Relative errors on the quantiles of peak flows and runoff volumes calculated from a UR and a NUR: influence of the runoff production parameter for the models 1 and 3.

Model 3 presents an intermediate behavior, which is in agreement with the way effective rainfall is calculated. The threshold effect, caused by the priority given to reservoir filling, is moderated by its variability over time, allowing runoff from the beginning of the rainfall. But, in so doing, the reservoir storage effect is effective for longer, and affects higher rainfalls. That is the reason why errors are bigger for rare events than in models 1 and 2, about −30 to −20%.

In any runoff production model, relative error decreases with an increase in cumulative frequency, which can be explained as follows: firstly, as seen earlier in models 1 and 3, the threshold effect of the runoff production model decreases towards the extreme events. Absolute errors vary little, thus relative errors decrease (see relative error definition: Eq. (2)); secondly, the biggest flows are generally obtained for rain events that affect the whole basin and have lower spatial heterogeneity of cumulative rainfall, and are therefore less sensitive to smoothing due to the spatial average. In the sample used, the three strongest peak flows calculated are due to very widespread events: these concern, respectively, 31, 37 and 16 out of 44 stations, where basin rainfall is over PMAX/2 (the median value is 4, cf. Table 1), and represent three out of four of the strongest basin rainfalls observed (81.2, 55.9 and 59.7 mm).

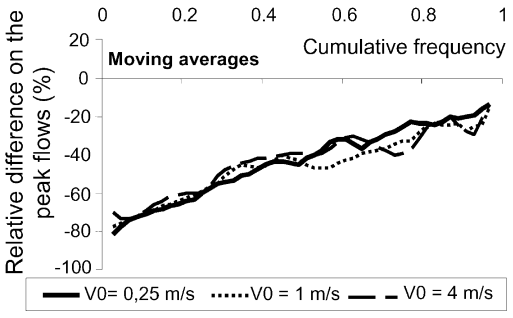

Fig. 7. Relative errors on the peak flows quantiles calculated from a UR and a NUR: influence of the routing model parameters.

3.1.2. Influence of the runoff production parameters

The conclusions did not change when parameters of the three runoff production models were modified. For Model 2, we checked that we obtained exactly the same relative errors regardless of the value represented by coefficient *W*. For the other models, comparison was made using STO = 10 mm (weak value) instead of the initial values (high value), STO = 20 mm for Model 1, STO = 30 mm for Model 3 (Fig. 6).

By increasing the effect of storage in Model 1, relative errors increase for frequent events, but remain identical for rare events. In the case of Model 3, the increase in error is constant (more or less 20%) over the whole range of cumulative frequencies. It can be thus concluded that the storage capacity of soil in a pure cumulative saturation soil process (Model 1) would have a strong effect overall on frequent events, whereas it affects rare events by means of some kind of Hortonian process (Model 3).

3.1.3. Influence of the routing model parameters

The influence of the routing model was analyzed by changing the value of the V0 parameter from 0.25 to 4 m/s (K0 = 0.7). This range of variation is large and arbitrary but it covers a wide range of situations that may be encountered. Production Model 3 was selected for the test, with STO = 30 mm.

Table 2
Characteristics of the four basins studied

	Basin 1	Basin 2	Basin 3	Basin 4
Surface area (km^2)	1531	383	103	22
Number of recording stations	44	20	6	4
R median (defined in Table 1)	3.4	2.7	1.6	1.4

The peak flow values do, of course, increase with transfer speed, but the relative errors presented in Fig. 7 remain very similar for each value of V0. This can be explained by the linearity of the routing model, which means that the peak flows are proportional to the runoff volumes: since runoff volume errors were not changed in the different tests because the same production model was used, linearity of the routing model ensures that peak flows error are identical. Using runoff production models 1 and 2 leads to the same conclusions.

In this part of the study, we were also interested in the influence of the time step on results. Calculations were thus carried out with a shorter time step (5 min), which gave the same results as with a 60 min time step. This is mainly due to the fact that the residence time in the basins studied is still much longer than the time step investigated. Any influence of the time step would only be effective if it exceeded the residence time. This may occur in a small basin with a high transfer speed, where the hourly time step is sometimes insufficient.

3.2. Influence of basin size

The basin that has been used for the simulations up to now is a relatively large basin (1531 km^2), in which the spatial variability of rainfall is documented by 44 rain gauges. In order to study the influence of basin size, we examined the results obtained using other smaller fictitious basins, whose characteristics are summarized in Table 2.

Comparison was performed using the 'intermediate' model: runoff production Model 3 with STO = 30 mm, V0 = 1 m/s and K0 = 0.7 for the routing model, and an hourly time step (Fig. 8).

It can be seen that the relative errors are generally much greater for the largest basins (1 and 2) than for the smallest (3 and 4), although there is a relative decrease in these differences towards the rare frequencies. This can be explained by the fact that the spatial variability of rainfall increases with catchment size. This result is in agreement with the assumption that the mean spatial extent of rainfall is around a few hundred square kilometers in the Mexico basin. This is also confirmed by the value of the range of the spherical variogram model, 30 km. In the same way, the analysis of the spatial coefficient of variation (CV_S) shows that mean values decrease from 0.73 to 0.29 with an increase in the size of the basin (Table 3). However, a bias may be caused by different number of rain gauges, which is very low in the smallest basins.

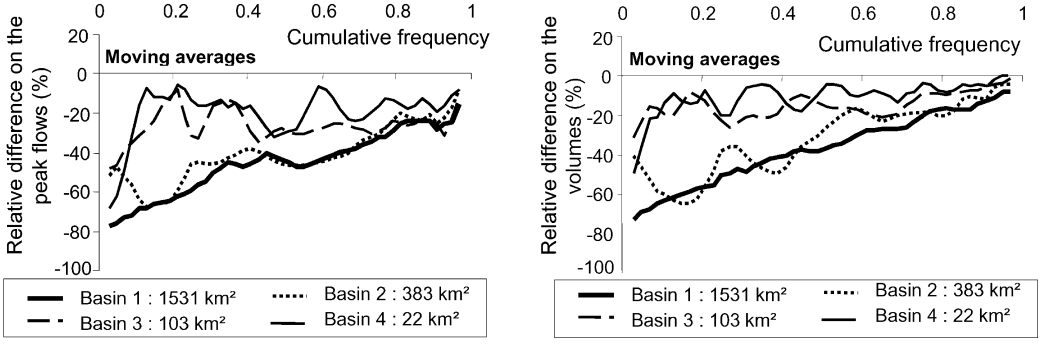

Fig. 8. Relative errors on the quantiles of peak flows and runoff volumes, calculated from a UR and a NUR: influence of basin size.

Table 3
Median CV_S values for station sampled

Basin size (km^2)	1531	383	103	22
CV_S median (all stations)	0.73 (basin 1)	0.67 (basin 2)	0.35 (basin 3)	0.29 (basin 4)
CV_S median (1 station out of 2)	0.72 (basin 1)	0.70 (basin 2)	0.32 (basin 3)	0.18 (basin 4)
CV_S median (median of 100 generated basins)	–	0.63	0.46	0.23
Range of CV_S median	–	0.55–0.67	0.32–0.61	0–0.46

Obviously, if this number is reduced to one, both relative errors and CV_S will be zero. Thus, CV_S were also calculated to account for only one gage out of two in each catchment, and it will be noted that their mean values do not change (Table 3), except in the smallest basin, where the number of stations is too small for a significant comparison. This proves that the spatial variability of the rainfall is correctly characterized by the existing stations, at least for basins 1, 2 and 3. Consequently, this variability really does increase with the size of the basin, and is the origin of differences in both volumes and peak flows as a function of either the UR and NUR patterns.

In addition, we studied the influence of the location of the fictitious basins on the determination of the CV_S. For basins 2, 3 and 4 (383, 103 and 22 km^2), we regularly moved the center of the basins in the study area to generate a representative sample of 100 basins of equal size. For each basin, it was shown that the median CV_S do not change Table 3), and that the intially selected basins are representative of the spatial variability of rainfall.

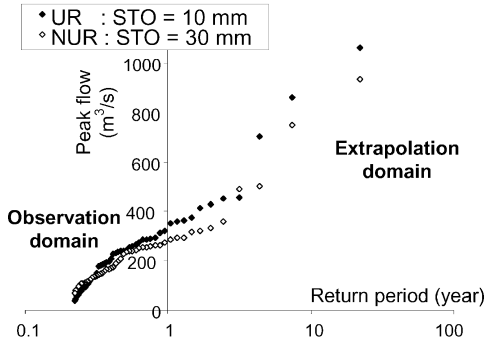

Fig. 9. Empirical probability distributions of the peak flows modeled from the sample of 50 rain events, using runoff production Model 3 and the parameters linked to the type of rainfall.

3.3. Influence on both calibration and extrapolation of a rainfall-runoff model

As mentioned earlier, the advantage of using rain fields in rainfall-runoff modeling is relatively weak in the case of extreme events. The error ranges from −30 to −10% depending on the hydrological model selected and the size of the basin. For current rainfall events, the differences are clearly more significant, about −80 to −20%. These differences must be taken into account, because they can have a very strong impact on both calibration and extrapolation of a rainfall-runoff model. Most of the time, calibration is indeed based on limited available information, generally frequent rainfall events. Thus significant errors may occur in the estimation of parameters with respect to the selected pattern of spatial variability of rainfall; and consequently, the extrapolation of the calibrated model may involve greater uncertainties towards the rare events.

As an example, let us consider as 'real' flow values calculated for the largest basin (1531 km^2), using an intermediate model (runoff production Model 3 with STO = 30 mm and V0 = 1 m/s, K0 = 0.7), an hourly time step, and the NUR pattern. Next, let us calibrate the same hydrological model to these flow values, but using the UR pattern. In order to be realistic, we also suppose that only a limited number of observations are available for calibration, for example those for which the return period is less than 1 year. Under these conditions, the calibration of the model using the UR pattern changed the parameter values significantly: among other possibilities, we obtained good results with STO = 10 mm, V0 = 1 m/s, K0 = 0.7. As can be seen in Fig. 9, the empirical distribution of the flows obtained with UR and STO = 10 mm coincides well with that of the flows obtained with a NUR and STO = 30 mm in the range of the flows for return periods of less than 1 year.

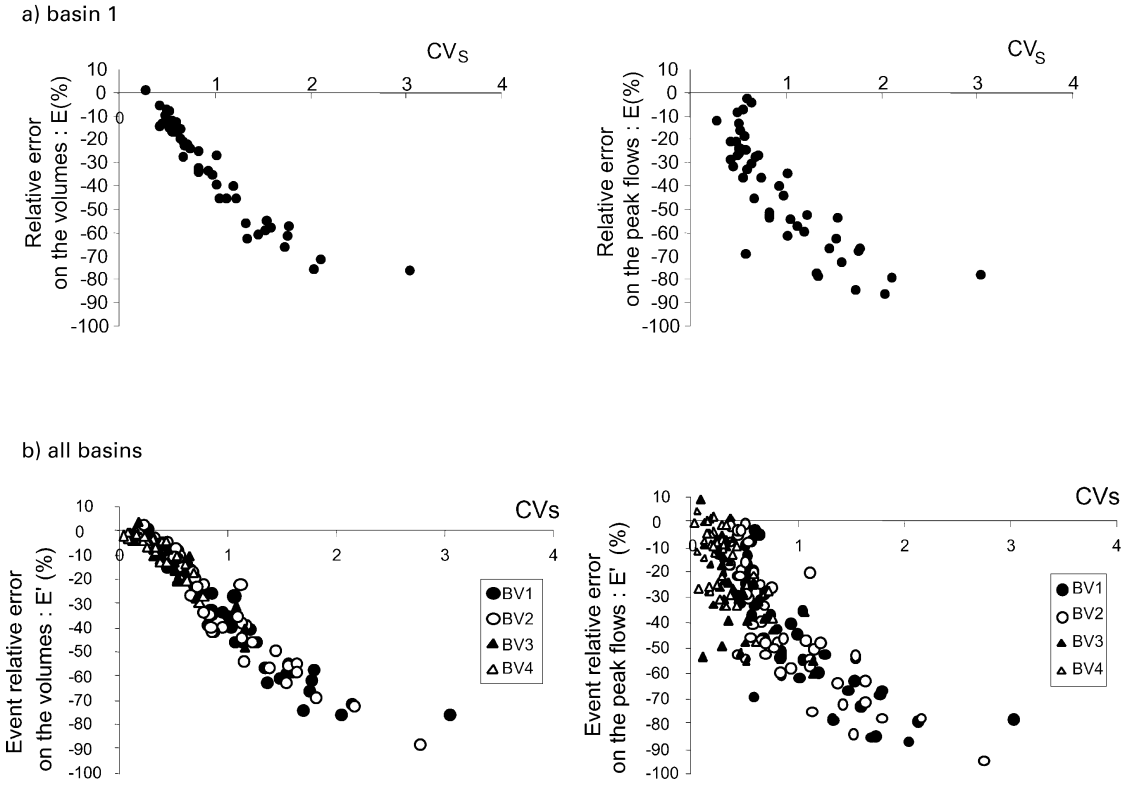

Fig. 10. Relationship between the relative error and the spatial coefficient of variation.

It will be noted that estimation of the STO parameter is greatly affected by the way the rainfall pattern is represented. The first problem consequently concerns the physical interpretation of the model parameter (here STO, but it could be any other parameter): how can STO be linked to physical indicators if it is so sensitive to the rainfall pattern? The second problem is connected with extrapolation of the model: it should be noted that divergences from 'real' flows appear in the case of higher return periods, and that flows calculated with STO = 10 mm and UR pattern are systematically over-estimated. This over-estimation presents maximum relative errors of about 30% for the return periods ranging from 1 to 10 years, and decreases in the case of the highest return periods.

From this example, we can conclude that calibrating a rainfall-runoff model using the UR pattern will have both a tendency to introduce a severe bias in the interpretation of model parameters, and to over-estimate rare frequency flows. However, we cannot generalize the degree of over-estimation, which depends to a large extent on both the hydrological processes and characteristics of the region studied.

3.4. Influence of the rainfields characteristics

As we have seen before, the distribution of both volumes and peak flows using either UR and NUR patterns is subject to variations that depend on the magnitude of spatial variability and on the return period of the event. But up to now, these variations have not been directly linked to any rainfields characteristics. This is the objective of this paragraph.

For the largest basin (1), we compared the (E_i') with the coefficients of variation (CV_i), given by Eq. (1). Comparison was performed using the intermediate model: runoff production Model 3 with STO = 30 mm, V0 = 1 m/s and K0 = 0.7 for the routing model, and an hourly time step (Fig. 10a). The relationships between (E_i') and (CV_i) are fairly good, a

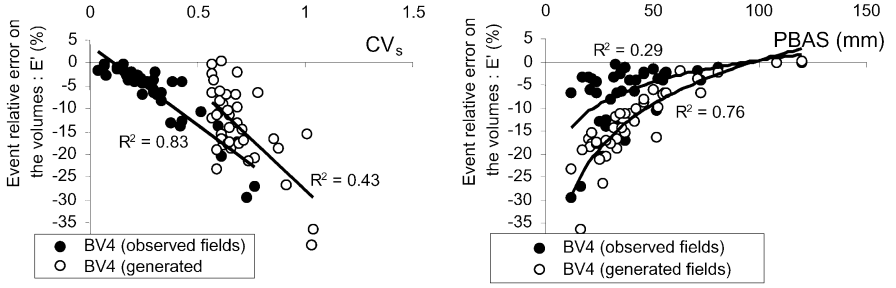

Fig. 11. Relationship between event relative error (E'), and respectively, CV_S and PBAS, from observed and generated fields.

little better for volumes than for peak flows. This can be explained by the fact that peak flows may be influenced by the position in time of the most intense storm (at the beginning or at the end of the event), whereas volumes are not. Furthermore, when considering all the basins on the same plot (Fig. 10b), it can be seen that the relationships do not change from a basin to another: this means that in a given model, the relationship is independent of the size of the basin. In the local context, the coefficient of variation can therefore be considered as a strong index of error at the event scale: with respect to the R^2 coefficient of determination of linear regressions, we found that the CV_S of the rain events explain 64% of the relative error (E')s on the peak flow, and 92% of the relative error on runoff volumes, for calculated flows using Model 3.

It is also important to check if this kind of relationship would change in the case of a different spatial structure of the rainfall fields, e.g. in other climatic contexts. We consequently generated new rain fields with the same spatial mean as the observed field, but with increased spatial variability. From the (NUR) hyetographs of each event, the new rain fields were generated at each grid mesh by multiplying rainfall with a randomized coefficient that derived from the uniform distribution, varying from 0 to 2. In this way we obtained very chaotic rain fields that may appear unrealistic, but are convenient for our given purpose.

Such simulation was carried out on the smallest basin (BV4). Runoff volumes were calculated using either UR or NUR rainfall patterns with the same rainfall-runoff modeling conditions as earlier. As can be seen in Fig. 11, we obtained a very different relationship than the previous one. The most important event of the sample (PBAS = 120 mm, CV observed field = 0.15, CV generated field = 0.67) is not very sensitive to the different UR and NUR patterns (E' is very close to zero in both cases), because the rain largely exceeds the threshold of 30 mm for a large number of grid meshes. Thus, in spite of the CV_S of the generated fields are much higher than those of the observed fields, the main factor that explains the relative error variability in this case is no longer CV ($R^2 = 0.43$), but ln(PBAS) ($R^2 = 0.76$). This example shows that the influence of PBAS is predominant, and must be taken into account in order to generalize the relationships between relative errors and rainfall characteristics.

In order to get a more general relationship, we then carried out multiple regressions between (E'), (PBAS) and (CV). Finally, the same linear relationship between $\ln(-E')$, CV and ln(PBAS) was proved to be satisfactory whether the fields are generated or observed:

$$\ln(-E') = 0.881 \ln(\mathrm{CV}) - 0.031\mathrm{PBAS} - 0.648 \quad (3)$$

Fitting of the relationship can be characterized through the differences between observed values (x) of the errors $\ln(-E')$ and predicted values (y) by the model, these are:

BV4 observed fields $y = 0.98x$ $\quad R^2 = 0.79$

BV4 generated fieds $y = 0.95x$ $\quad R^2 = 0.71$

Applications to the observed events of the other basins show that Eq. (3) is still convenient, since the maximal bias (in BV1) remains smaller than 16%:

BV3 observed fields $y = 1.00x$ $\quad R^2 = 0.85$

BV2 observed fields $y = 1.05x$ $R^2 = 0.95$

BV1 observed fields $y = 1.16x$ $R^2 = 0.95$

The relationship may therefore give a first estimation of the error associated with the runoff volumes, for a given model. However, Eq. (3) must only be considered as indicative and a further perspective consists in checking its validity in other contexts.

The same procedure was applied to the peak flows, but no satisfactory relationship between E', PBAS and CV could be adjusted, probably because the position of the most intense rainfall inside the whole event must also be taken into account.

4. Discussion

It should be possible to extrapolate the results we obtained to the areas with equivalent spatial and temporal rainfall characteristics. Both tropical and equatorial mountainous sites may be considered. Moreover, the relationship between the calculated relative errors and the rainfall characteristics means it is possible to envisage the results that would be obtained in other conditions of rainfall spatial variability. However, such relationship depends on both the selected runoff model and the value of its parameter. A rainfall simulation model would be very useful to explore the sensitivity of the hydrological models under a large array of rainfall, and this must now be undertaken.

This study was based on some simplified assumptions. Although we neither consider the spatial variability of runoff production parameters, nor their temporal variability (for example related to initial soil moisture conditions), it is possible to show what effects would be caused by doing so.

In case of the initial moisture conditions, which were fixed at zero at the beginning of each event, using a higher value would be equivalent to reducing the STO value for models 1 and 3. And, as was shown in Section 3.1.2, this would also reduce the relative errors caused by using the UR pattern instead of the NUR one. However, in the tropical context, evapotranspiration is generally very high between rainy events, and the intervals between events are usually long enough to ensure that low initial soil moisture conditions predominate. Thus any overestimation of the errors due to the assumption of dry initial conditions is probably slight.

The other simplified assumptions we made (spatial uniformity of the production model parameters, final infiltration to zero, absence of percolation or evapotranspiration at the event scale, linearity of the routing model) on the other hand, tend to underestimate the relative errors. The influence of these assumptions requires further study. Nevertheless, it can be deduced that in the case of extreme events results will generally be little affected by these assumptions, and if this is the case, we can conclude that the UR rainfall variability pattern is acceptable for estimating the frequency of extreme floods. In such a case, design rainfall for the estimation of extreme flows could be based on point rainfall distribution combined with the areal reduction factor. In Mexico's climatic context, this assumption seems to concern a rather large range of both models and surface areas.

5. Conclusion

Using a sample of 50 rain events from a dense rain gauge network around Mexico City, we studied the influence of the spatial variability of rainfall on the estimation of both peak flows and runoff volumes. These were calculated from distributed hydrological models using different patterns of rainfall representation as input data: spatially averaged UR, and NUR.

Both calculated runoff volumes and flows can differ considerably as a function of these two patterns, depending on the selected runoff production model, the size of the catchment, and the frequency of the event. Runoff production models based on storage reservoirs are the most sensitive. Differences increase with the size of the catchment because there is also an increase in rainfall variability of rainfall. In general, for any model and any basin area, the differences are less for extreme events than for current rainfall events. To sum up, relative errors vary from -30 to -10% for the former and from -80 to -20% for the latter. There are two reasons for this: firstly, in the local context the most significant flows are generated by widespread rainfalls, and secondly the effect of storage associated with models 1 and 3 is strongly mitigated for the highest rainfalls.

Two main conclusions can be drawn in the local context of this study. First, given the moderate influence of rainfall variability patterns on extreme events, in most cases design storms do not need to respect the whole rain field, but can be derived from statistics at a given point and combined with the probabilistic concept of the areal reduction factor. Second, the calibration of a rainfall-runoff model can be severely affected when using a spatially averaged rainfall instead of a rain field. Generated biases have consequences for the numerical stability of the model parameters from one event to another and consequently on the overall and physical interpretation of these parameters. Furthermore, rare and extreme flows are generally overestimated. In the example that we presented, overestimation reached 30% for return periods ranging between 2 and 5 years, a little less for higher return periods.

Although these differences did not reach exceptional values, attention must be paid to errors caused by not taking spatial rainfall organization into account in the hydrological models. It should also be noted that, in this study, some simplified assumptions concerning the basins (spatial uniformity of the morphological and physiographical factors) and the models used (no continuous infiltration, linear routing model) may underestimate the influence of the spatial organization of rainfall. Consequently we recommend that this kind of study be carried out for real catchments (using other parameters or models), and also in other climatic regions.

Acknowledgements

The authors thank Dr Thierry Lebel and Dr Murugesu Sivapalan for providing helpful suggestions for improving the manuscript. This work has been performed within a project developed by IRD (Institut de Recherche pour le Développement, France) and UNAM (Universidad Nacional Autonoma de Mexico, Instituto de Ingenieria), and was funded by CONACYT in Mexico.

References

Bell, T.L., 1987. A space-time stochastic model of rainfall for satellite remote-sensing studies. J. Geophys. Res. 92 (8), 9631–9643.

Bouvier, Ch., Delclaux, F., 1996. ATHYS: a hydrological environment for spatial modelling and coupling with a GIS. Proceedings of the HydroGIS 96, Vienna, Austria, pp. 19–28. IAHS publication no 235.

Bouvier, C., Fuentes, G., Dominguez, R., 1994. Mercedes: un modèle hydrologique danalyse et de prévision de crues en milieu hétérogène. Crues et Inondations, 23èmes journées de lhydraulique, SHF, Nîmes, 14–16 September 1994, pp. 257–260.

Bouvier, C., Ayabaca, E., Perrin, J.L., Cruz, F., Fourcade, B., Rosario, S., Carrera, L., 1999. Variabilités temporelle et spatiale des averses en milieu andin: exemple de la ville de Quito (Equateur). Revue de Géographie Alpine 3 (87), 51–66.

Brunet-Moret, Y., Roche, M., 1966. Etude théorique et méthodologique de labattement des pluies. Cahiers ORSTOM: Série Hydrologie (FRA) 3 (4), 3–13.

Chocat, B. 1997. Encyclopédie de l'hydrologie urbaine et de l'assainissement, Eurydice92, Collection Technique and Documentation, Lavoisier.

Cisneros, L., Bouvier, C., Dominguez, R., 1998. Aplicacion del metodo kriging en la construccion de campos de tormenta en la Ciudad de Mexico. 18è Congreso LatinoAmericano de Hidraulica, Octubre 1998, Oaxaca, Mexico, pp. 379–388.

Cisneros, L., Bouvier, C., Dominguez, R., 2000. Generacion de campos de precipitacion en el Valle de Mexico. 19è Congreso LatinoAmericano de Hidraulica, Octubre 2000, pp. 249–258.

Creutin, D., Obled, C., Tourasse, P., 1980. Analyse spatiale et temporelle des épisodes pluvieux cévennols. La Météorologie, 6ème série 20–21, 233–242.

Dawdy, D.R., Bergman, J.M., 1969. Effect of rainfall variability on streamflow simulation. Water Resour. Res. 5, 958–969.

Faurés, J.M., Goodrich, D.C., Woolhiser, D.A., Sorooshian, S., 1995. Impact of small scale spatial rainfall variability on runoff modeling. J. Hydrol. 173, 309–326.

Goovaerts, P., 2000. Geostatistical approaches for incorporating elevation into the spatial interpolation of rainfall. J. Hydrol. 228 (1–2), 113–129.

Gupta, V.K., Waymire, E.C., 1979. A stochastic kinematic study of subsynoptic space-time rainfall. Water Resour. Res. 15, 637–644.

Krajewski, F.W., Lakshmi, V., Georgakakos, K.P., Jain, S.C., 1991. A Monte Carlo study of rainfall sampling effect on a distributed catchment model. Water Resour. Res. 27 (1), 119–128.

Kuczera, G., Williams, B.J., 1992. Effect of rainfall errors on accuracy of design flood estimates. Water Resour. Res. 28 (4), 1145–1153.

Lebel, T., Laborde, J.P., 1988. A geostatistical approach for areal rainfall statistics assessment. Stochastic Hydrol. Hydraul. 2, 245–261.

Maidment, D., 1993. Handbook of Hydrology. McGraw-Hill, New York.

Marshall, R.J., 1980. The estimation and distribution of storm movement and storm structure, using a correlation analysis technique and rainfall-gauge data. J. Hydrol. 48, 19–39.

Morin, J., Rosenfeld, D., Amitai, E., 1995. Radar rainfall field evaluation and possible use of its high temporal and spatial resolution for hydrological purposes. J. Hydrol. 172, 275–292.

Niemczynowicz, J., 1987. Storm tracking using raingauge data. J. Hydrol. 93, 135–152.

Niemczynowicz, J., 1991. On the storm movement and its applications. Atmos. Res. 27, 109–127.

Obled, Ch., Wendling, J., Beven, K., 1994. The sensibility of hydrological models to spatial rainfall patterns: an evaluation using observed data. J. Hydrol. 159, 305–333.

Rodriguez-Iturbe, I., Eagleson, P.S., 1987. Mathematical models of rainstorm events in space and time. Water Resour. Res. 23, 181–190.

Rodriguez-Iturbe, I., Mejia, J.M., 1974. On the transformation of point rainfall to areal rainfall. Water Resour. Res. 10, 729–735.

Sivapalan, M., Blöschl, G., 1998. Transformation of point rainfall to areal rainfall: intensity–duration–frequency curves. J. Hydrol. 204 (1–4), 150–167.

Sivapalan, M., Wood, E.F., 1987. A multidimensional model of nonstationary space-time rainfall at the catchment scale. Water Resour. Res. 23, 1289–1299.

Smith, J.A., Karr, A.F., 1985. Parameter estimation for a model of space-time rainfall. Water Resour. Res. 21 (8), 1251–1257.

Surkan, A.J., 1974. Simulation of storm velocity effects on flow from distributed channel networks. Water Resour. Res. 10 (6), 1149–1160.

Troutman, B., 1983. Runoff predictions errors and bias in parameters estimation induced by spatial variability of precipitation. Water Resour. Res. 19 (3), 791–810.

Waymire, E., Gupta, V.K., Rodriguez-Iturbe, I., 1984. A spectral theory of rainfall intensity at meso-beta scale. Water Resour. Res. 20, 1453–1465.

Wilson, C.B., Valdes, J.B., Rodriguez-Iturbe, I., 1979. On the influence of the spatial distribution rainfall on storm runoff. Water Resour. Res. 15 (2), 321–328.

Wotling, G., Bouvier, Ch., Danloux, J., Fritsch, J.-M., 2000. Regionalization of extreme precipitation distribution using the principal components of the topographical environment. J. Hydrol. 233, 86–101.

Yoo, C., Valdes, J.B., North, G.R., 1996. Stochastic modeling of multidimensional precipitation fields considering spectral structure. Water Resour. Res. 32 (7), 2175–2187.